



## Research Paper

**Cite this article:** Pezhman MM, Heidari AA, Ghafoorzadeh-Yazdi A, Homayoon F, Shahraki H (2024) A low-profile SIW multi-beam antenna array fed by a compact two-layer  $6 \times 6$  BFN. *International Journal of Microwave and Wireless Technologies* **16**(4), 559–566. <https://doi.org/10.1017/S1759078723001125>

Received: 27 May 2023

Revised: 10 September 2023

Accepted: 18 September 2023


### Keywords:

5G applications;  $6 \times 6$  BFN; beamforming network; hybrid coupler; interlayer crossover; multi-aperture couplers; multibeam antenna; phase shifter; SIW-technology; slot array

**Corresponding author:** Abbas Ali Heidari;

Email: [aheidari@yazd.ac.ir](mailto:aheidari@yazd.ac.ir)

# A low-profile SIW multi-beam antenna array fed by a compact two-layer $6 \times 6$ BFN

Mohammad Mahdi Pezhman<sup>1,2</sup>, Abbas Ali Heidari<sup>1</sup> , Ali Ghafoorzadeh-Yazdi<sup>1</sup>, Fatemeh Homayoon<sup>1</sup> and Hamed Shahraki<sup>3</sup>

<sup>1</sup>Department of Electrical Engineering, Yazd University, Yazd, Iran; <sup>2</sup>Department of Electrical Engineering, Vali-e-Asr University, Rafsanjan, Iran and <sup>3</sup>Department of Electrical Engineering, Velayat University, Iranshahr, Iran

## Abstract

This paper presents a low-profile six-beam antenna implemented by a compact two-layer  $6 \times 6$  beamforming network (BFN) and a  $6 \times 2$  slot antenna in substrate integrated waveguide (SIW) technology. The main components of the proposed  $6 \times 6$  BFN are  $3 \times 3$  multi-aperture couplers, interlayer hybrid couplers, and several phase shifters which are embedded on two microwave substrates. The proposed antenna has been designed, simulated, and fabricated for the frequency range of 28–32 GHz. The size of this antenna is  $82 \times 31.8 \times 0.787$  mm<sup>3</sup>, which can be a suitable choice for 5G applications due to its compact dimensions compared to similar works. Prototype testing shows that the proposed structure presents a stable beamforming performance both in simulation and measurement with good agreement. The antenna generates six radiation beams in directions  $\pm 9^\circ$ ,  $\pm 30^\circ$ , and  $\pm 54^\circ$  with good return losses and isolations.

## Introduction

In recent years, multi-beam antennas (MBAs) with passive beamforming networks (BFNs) have received attention for 5G/6G wireless communications [1–5]. Substrate integrated waveguide (SIW) combines the advantages of the conventional waveguide and the microstrip line, presenting low-profile, high-quality factor, low transmission loss, and easy processing characteristics. So, MBAs with SIW lines have been quickly developed. Various structures of BFNs such as quasi-optical networks and circuit BFNs are employed to achieve desired amplitude and phase for multi-beam applications. The quasi-optical structures such as Ruze and Rotman lenses [6–8] are not suitable for high-power applications. Therefore, circuit BFNs such as Nolen matrix [9], Blass matrix [10], and Butler matrix [11] based on various couplers, crossovers, and phase shifters are mostly used in MBA designs. Among circuit BFNs, Butler matrix is preferred over other techniques, because it requires the least number of components and employs fewer phase shifters than the Nolen and Blass matrices. For 5G applications, different types of Butler matrices have been proposed such as  $4 \times 4$  SIW Butler matrix [12, 13]. In its conventional form, the Butler matrices are usually designed in the  $4 \times 4$  [14, 15],  $8 \times 8$  [16], and  $16 \times 16$  [17, 18] forms which can only feed  $2^n$  radiation elements ( $n = 1, 2, 3, \dots$ ). Of course, some BFNs have been suggested with the desired number of beams. For example, a SIW seven-beam antenna based on a Rotman lens, and a modified SIW R-KR lens with 15 radiation beams are presented in papers [19] and [20], respectively. However, the losses of these BFNs are relatively high and they also have a narrow frequency bandwidth compared to circuit BFNs, especially the Butler matrix. Recently, many research works have been carried out to overcome the limitation of the number of beams of the Butler matrix. In paper [21], a compact SIW  $3 \times 3$  Butler matrix is designed with a combination of hybrid couplers and phase shifters for 5G mobile applications. Although the designed Butler matrix creates three radiation beams, its dimensions are relatively large. Some works with different numbers of inputs and outputs are also presented including  $5 \times 6$  Butler matrix with circular polarization [22],  $4 \times 8$  Butler matrix with side-lobe suppression [23], and 2-D scanning multi-beam array utilizing  $9 \times 3$  BFN [24]. Recently, to increase the possible number of beams and reduce the dimensions of the BFNs, applying couplers with junctions more than the hybrid coupler, such as  $3 \times 3$  and  $4 \times 4$  multi-aperture couplers (MACs), were proposed in papers [25–27]. According to Kim et al. [28], a new method was proposed to create six radiation beams. This work presents a novel single layer  $6 \times 6$  circuit BFN consisting of several  $3 \times 3$  MACs, hybrid couplers, crossovers, and phase shifters. Miniaturization of BFNs especially Butler matrix is a required in millimeter-wave multi-beam applications. Layering the structure is one of the methods to miniaturize the size of BFNs. In the last decade, many Butler matrices have been proposed using multilayer configurations [28–30].

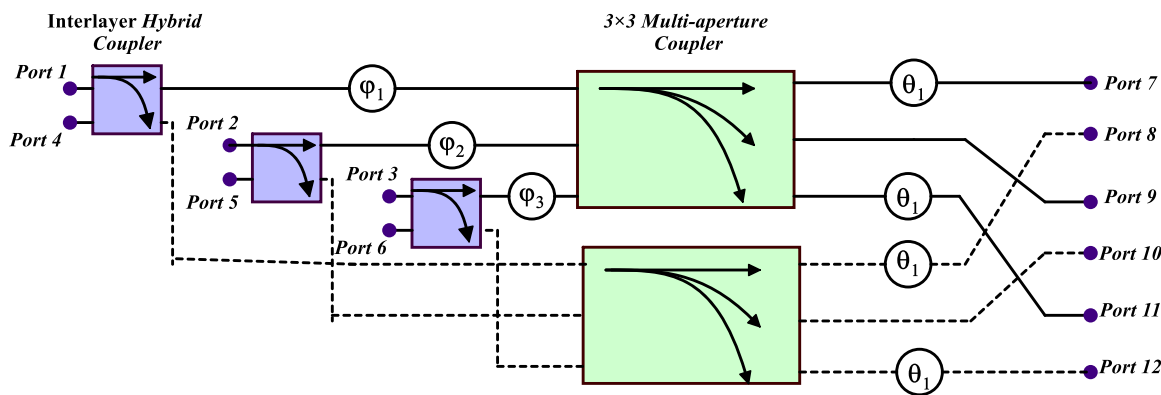


**Figure 1.** Block diagram of the proposed two-layer 6 × 6 BFN. (The dashed lines are on the bottom layer).

In the present study, a low-profile SIW MBA fed by a compact two-layer 6 × 6 BFN is proposed. According to the theory of uniform array antennas [31], to produce six radiation beams using six linear elements, a BFN with the ability to distribute power with equal amplitudes and phase differences of ±30°, ±90°, and ±150° is required. The conventional Butler matrix is not able to realize these amplitudes and phases. As explained in paper [32], to realize 6 × 6 BFN, 3 × 3 MACs can be combined with hybrid couplers and phase shifters. In this paper, to present a compact 6 × 6 BFN, two 3 × 3 couplers placed on separate layers are used. Of course, other passive components such as hybrid couplers and phase shifters are also used to achieve the desired amplitudes and phases. The proposed BFN is simpler than similar structures due to the use of fewer components. Especially, by eliminating crossovers in the proposed BFN, the complexity of the structure has been reduced. Since crossover manufacturing is a bit complicated, its design needs more precision [33]. Also, crossover is an element that has a good performance only in the central frequency and may not have a good output across the frequency bandwidth of the BFN. So, by eliminating the crossover, it is possible to achieve more flat amplitudes and phases in the BFN outputs. The operating frequency band of the proposed design is from 28 to 32 GHz, which is suitable for 5G applications. Six radiation beams with a stable realized gain around 13 dBi are produced in directions ±9°, ±30°, and ±54°. Details of the paper are organized as follows:

The design process of the proposed 6 × 6 BFN is given in the following section. The fabricated prototype of the proposed six-beam antenna and experimental results are presented in the “Antenna fabrication and measurement results” section, and conclusions for this study are provided in the “Conclusion” section.

### Design process of the 6 × 6 two-layer BFN

According to the theory of uniform array antennas, to generate six radiation beams, a BFN is needed that can excite the array antenna elements with equal amplitudes and phase differences of ±30°, ±90°, and ±150° [32]. In this section, in order to realize these values, a 6 × 6 two-layer BFN is designed. Obviously, 3 × 3 MACs can be an appropriate choice for a six-beam BFN. In the proposed structure, to miniaturize the 6 × 6 BFN, two microwave layers are used, and the main component of each layer is a 3 × 3 MAC. Of course, other components such as 90° hybrid couplers and phase shifters are also used to achieve the desired

amplitudes and phases. Figure 1 shows the block diagram of the proposed 6 × 6 two-layer BFN. This BFN has six input ports (ports 1–6) and six output ports (ports 7–12). Ports 1–3 and ports 4–6 are considered as top layer inputs and bottom layer inputs, respectively.

The proposed topology is such that by exciting each input port, the power is first distributed between two layers with equal amplitude (1/2 ratio) and 90° phase difference, by interlayer hybrid couplers. Then, each layer divides its received power equally between the outputs using the 3 × 3 MAC (1/3 ratio). Therefore, the condition of equal power distribution (dividing the input power with a ratio of 1/6) between the outputs has been realized, which is known as the first feature of BFNs. Suitable phase shifters have been embedded to achieve the second condition of the 6 × 6 BFN, i.e. phase difference of ±30°, ±90°, and ±150° between the successive outputs. In the following sections, the theory of the proposed two-layer 6 × 6 BFN and the implementation of its components using SIW transmission lines are given.

### Theory of the proposed BFN

As mentioned in the previous section and shown in Fig. 1, the 3 × 3 MAC is the main component of the proposed 6 × 6 BFN. The design process of the 3 × 3 coupler and its features are presented in paper [25]. However, the performance of this coupler can be summarized according to Table 1.

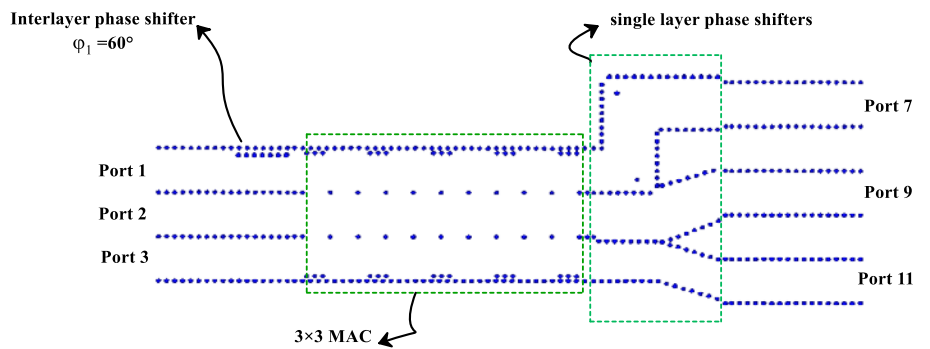
The hybrid couplers also distribute their input power with an equal ratio and a 90° phase difference between their outputs. According to the phases generated by 3 × 3 couplers and hybrid couplers, the output phases of the proposed BFN (phases of ports 7–12 in Fig. 1) are obtained according to Table 2. As can be seen in Fig. 1, to adjust the output phase differences on desired values, phase shifters  $\varphi_1$ ,  $\varphi_2$ ,  $\varphi_3$ , and  $\theta_1$  have been added in the structure of

**Table 1.** Amplitude and phase of 3 × 3 MAC outputs (phase reference is Output 1)

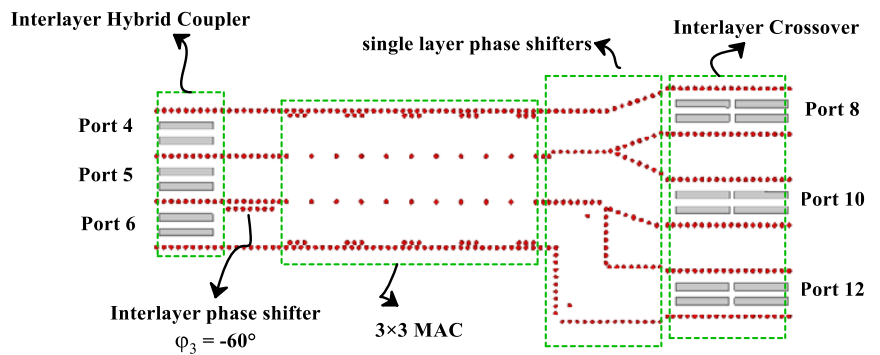
Excited port	Output 1	Output 2	Output 3
Port 1	$1/3 e^{j0}$	$1/3 e^{-j150}$	$1/3 e^{-j240}$
Port 2	$1/3 e^{j0}$	$1/3 e^{-j30}$	$1/3 e^{j0}$
Port 3	$1/3 e^{j0}$	$1/3 e^{+j90}$	$1/3 e^{+j240}$

**Table 2.** Output phases of the proposed 6 × 6 BFN based on the excitation of input ports

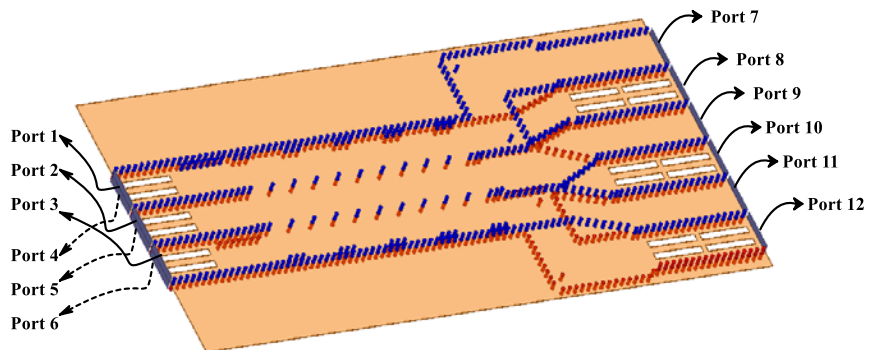
	Port 7	Port 8	Port 9	Port 10	Port 11	Port 12
Port1	$\varphi_1 + \theta_1$	$-90 + \theta_1$	$\varphi_1 - 150$	$-90-150$	$\varphi_1 - 240 + \theta_1$	$-90 - 240 + \theta_1$
Port 2	$\varphi_2 + \theta_1$	$-90 + \theta_1$	$\varphi_2 - 30$	$-90-30$	$\varphi_2 + \theta_1$	$-90 + \theta_1$
Port 3	$\varphi_3 + \theta_1$	$-90 + \theta_1$	$\varphi_3 + 90$	$-90+90$	$\varphi_3 + 240 + \theta_1$	$-90 + 240 + \theta_1$
Port 4	$-90 + \varphi_1 + \theta_1$	$\theta_1$	$-90 + \varphi_1 - 150$	$-150$	$-90 + \varphi_1 - 240 + \theta_1$	$-240 + \theta_1$
Port 5	$-90 + \varphi_2 + \theta_1$	$\theta_1$	$-90 + \varphi_2 - 30$	$-30$	$-90 + \varphi_2 + \theta_1$	$\theta_1$
Port 6	$-90 + \varphi_3 + \theta_1$	$\theta_1$	$-90 + \varphi_3 + 90$	$+90$	$-90 + \varphi_3 + 240 + \theta_1$	$+240 + \theta_1$



(a)



(b)



(c)

**Figure 2.** SIW-proposed BFN: (a) top layer, (b) bottom layer, and (c) 3D view.

the proposed BFN. Phase shifters  $\varphi_1, \varphi_2$ , and  $\varphi_3$  create a phase difference between each path of the top layer with its adjacent path at bottom layer. Phase shifter  $\theta_1$  generates a phase difference between outputs of the  $3 \times 3$  MACs used in the top and bottom layers. By exciting port 1, the phase difference of successive outputs can be calculated according to the following relations:

$$\begin{aligned} \Delta\varphi_{7,8} &= \varphi_1 + 90^\circ \\ \Delta\varphi_{8,9} &= \theta_1 - \varphi_1 + 60^\circ \\ \Delta\varphi_{9,10} &= \varphi_1 + 90^\circ \\ \Delta\varphi_{10,11} &= -\varphi_1 - \theta_1 \\ \Delta\varphi_{11,12} &= \varphi_1 + 90^\circ \end{aligned} \quad , \quad \Delta\varphi_{i,j} = \angle port_i - \angle port_j \quad (1)$$

where  $\Delta\varphi_{i,j}$  is equal to the phase difference between port  $i$  and port  $j$ . In the proposed BFN, when port 1 is excited, the phase difference of the outputs should be equal to  $150^\circ$ . As a result,  $\varphi_1$  and  $\theta_1$  can be concluded according to Eq. (2):

$$\begin{aligned} \Delta\varphi_{7,8} &= \Delta\varphi_{8,9} = \Delta\varphi_{9,10} = \Delta\varphi_{10,11} = \Delta\varphi_{11,12} \\ &= 150^\circ \Rightarrow \varphi_1 + 90^\circ = \theta_1 - \varphi_1 + 60^\circ = \varphi_1 + 90^\circ \\ &= -\varphi_1 - \theta_1 = \varphi_1 + 90^\circ = 150^\circ \Rightarrow \varphi_1 = 60^\circ, \theta_1 = 150^\circ \end{aligned} \quad (2)$$

Similarly, for the excitation of port 2, the phase difference of the outputs should be equal to  $90^\circ$ :

$$\begin{aligned} \Delta\varphi_{7,8} &= \Delta\varphi_{8,9} = \Delta\varphi_{9,10} = \Delta\varphi_{10,11} = \Delta\varphi_{11,12} \\ &= 90^\circ \Rightarrow \varphi_2 + 90^\circ = \theta_1 - \varphi_2 - 60^\circ = \varphi_2 + 90^\circ \\ &= -120^\circ - \varphi_2 - \theta_1 = \varphi_2 + 90^\circ \\ &= 90^\circ \Rightarrow \varphi_2 = 0^\circ, \theta_1 = 150^\circ \end{aligned} \quad (3)$$

If port 3 is excited the output phase difference should be set to  $30^\circ$ :

$$\begin{aligned} \Delta\varphi_{7,8} &= \Delta\varphi_{8,9} = \Delta\varphi_{9,10} = \Delta\varphi_{10,11} = \Delta\varphi_{11,12} \\ &= 30^\circ \Rightarrow \varphi_3 + 90^\circ = \theta_1 - \varphi_3 - 180^\circ = \varphi_3 + 90^\circ \\ &= -240^\circ - \varphi_3 - \theta_1 = \varphi_3 + 90^\circ \\ &= 30^\circ \Rightarrow \varphi_3 = -60^\circ, \theta_1 = 150^\circ \end{aligned} \quad (4)$$

Due to the symmetry in the proposed structure, by exciting ports 4–6, the output phase differences are set to the values of  $-30^\circ$ ,  $-90^\circ$ , and  $-150^\circ$ , respectively.

### Two-layer BFN implementation by SIW-lines

Figure 2 shows the structure of the proposed BFN implemented using SIW-lines.

As can be seen in Fig. 2, the components of the proposed dual-layer BFN include interlayer hybrid couplers,  $3 \times 3$  MACs, interlayer crossovers,  $60^\circ$  interlayer phase shifter,  $-60^\circ$  interlayer phase shifter, and single-layer phase shifters. The design process of the SIW  $3 \times 3$  MAC and its simulation results are completely given in our previous work in paper [25]. According to the presented theory, the interlayer hybrid couplers should be able to distribute the input power between the two layers with equal amplitude and  $90^\circ$  phase difference. This feature is realized by using the

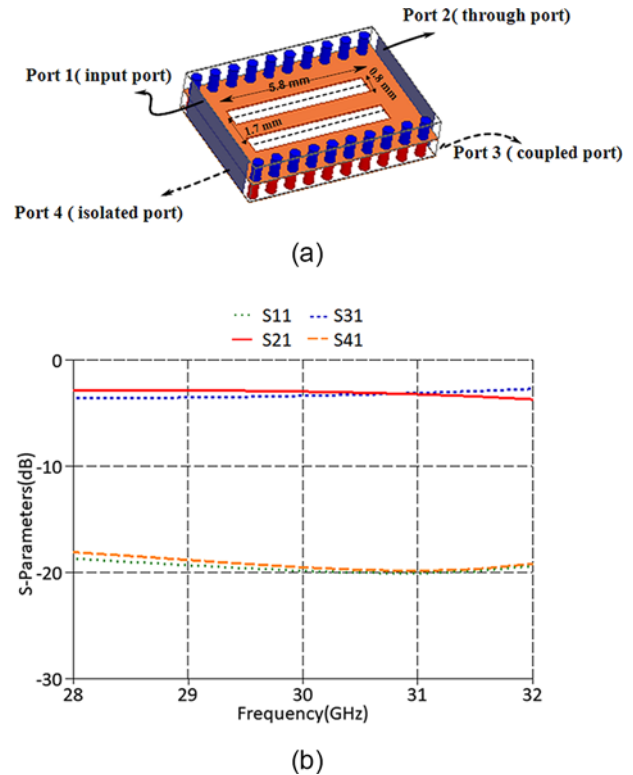


Figure 3. (a) Structure of the SIW interlayer hybrid coupler, and (b) simulation results.

slots that are embedded between the two layers. The SIW interlayer hybrid coupler and simulation results are shown in Fig. 3(a) and (b), respectively. The simulated S-parameters show that by exciting each input port of this coupler (e.g., port 1), the power is almost equally divided between the through and coupled ports ( $|S_{21}| = |S_{31}| \cong 3$  dB) and there is a good return loss and isolation between the input and isolated ports.

Two types of phase shifters are used in the proposed structure: interlayer phase shifters that create a phase difference between the top and bottom layers, and single-layer phase shifters that are used separately in each layer and create a phase difference between the paths of each layer. The  $60^\circ$  interlayer phase shifter should be generated a  $60^\circ$  phase difference between the paths caused by the exciting of ports 1 and 4. As can be seen in Fig. 2, this phase difference is produced using “equal length unequal width lines”. Similarly, by placing these lines in the path of the bottom layer,  $-60^\circ$  phase difference is generated between ports 3 and 6. Finally, to realize the desired phase difference and also to place all the output ports on the same level (to connect the BFN to a broadside array antenna), single-layer phase shifters are designed in the top and bottom layers according to Fig. 2(a) and (b), respectively.

Several crossovers are used at the end of the bottom layer so that the power of this layer is coupled to the top layer. Also, two hybrid couplers have been cascaded to implement the crossover. The proposed BFN (Fig. 2(c)) is simulated by HFSS software and its S-parameters are obtained according to Fig. 4. As can be seen in graphs of Fig. 4, in the frequency range of 28–32 GHz, by exciting each of the ports 1–3, the input power is distributed almost equally between the BFN outputs (ratio of 1/6 or  $-7.8$  dB). Also, the return loss and isolation between the inputs have desirable values. Due to

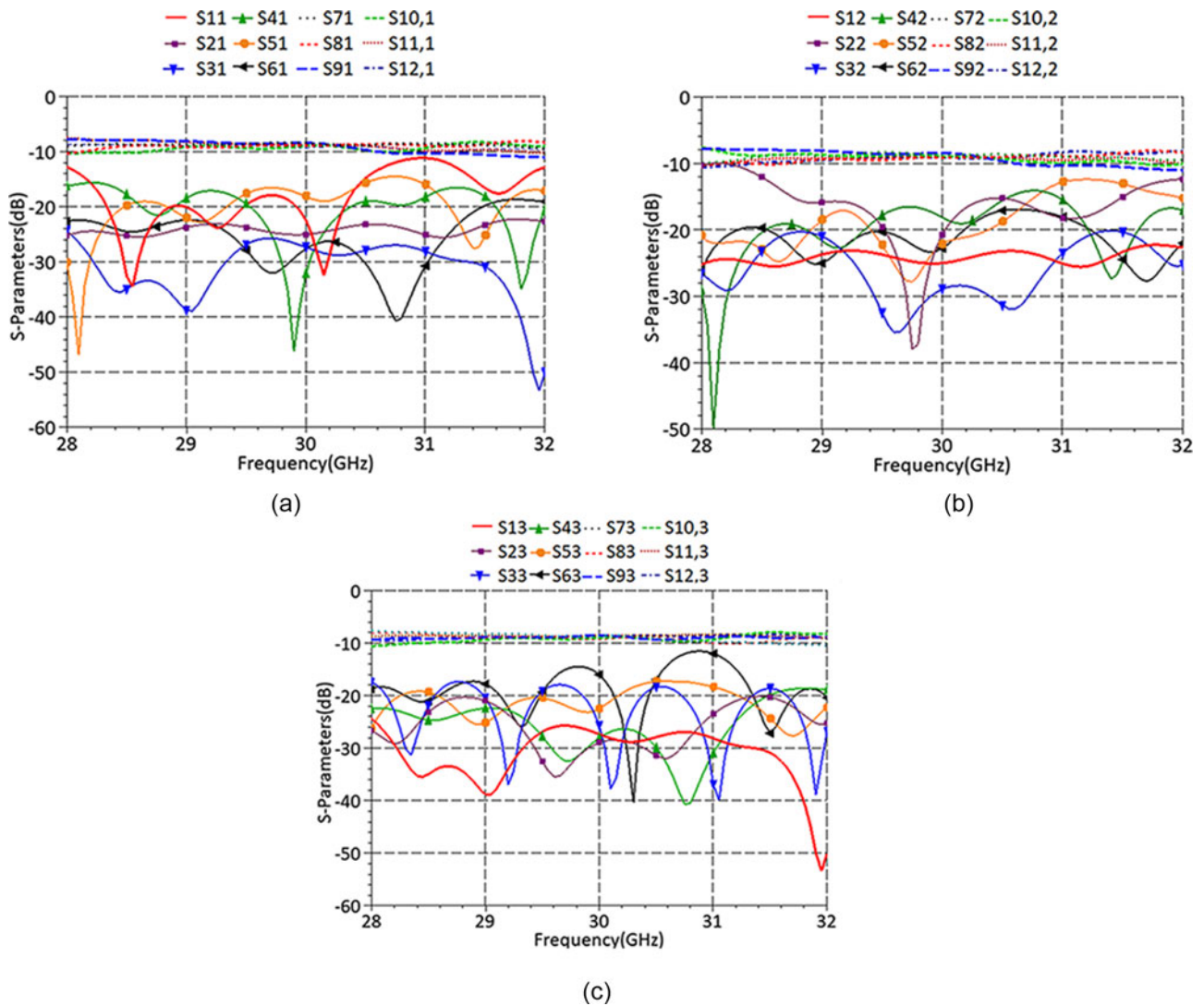


Figure 4. Simulated S-parameters of the proposed two-layer BFN: (a) excitation of port 1, (b) excitation of port 2, and (c) excitation of port 3.

the similarity of the top layer and the bottom layer, the simulation results for the excitation of ports 4–6 are also similar to those of ports 1–3.

Figure 5 shows the phase differences of successive outputs when ports 1–3 of the proposed BFN are excited. At the central frequency ( $f = 30$  GHz), the simulated phase differences are approximately equal to the values of  $+150^\circ$ ,  $+90^\circ$ , and  $+30^\circ$  for the excitation of ports 1–3, respectively. Due to the symmetry in the proposed structure, these phase differences for ports 4–6 are about  $-30^\circ$ ,  $-90^\circ$ , and  $-150^\circ$ , respectively. By comparing these values with the theoretical results, it can be concluded that the proposed structure has produced the necessary phase differences to create six radiation beams.

### Antenna fabrication and measurement results

As explained in the previous section, the outputs of the bottom layer are transferred to the top layer so that all outputs are placed on the same level. In this case, this BFN can be connected to the SIW slot arrays. We use a  $6 \times 2$ -slot array antenna

with a similar design process to the array antenna presented in paper [32]. The fabricated prototype of the proposed two-layer six-beam antenna is shown in Fig. 6. This antenna is fabricated and assembled using Rogers RT/duroid 5870 substrate with a thickness of 0.787 mm, a dielectric constant of 2.33, and a loss tangent of 0.0012.

The simulated and measured S-parameters of the six-beam antenna were achieved by HFSS V17.0 and an Agilent network analyzer, respectively. Also, the radiation patterns and gains are measured in an anechoic chamber. The simulated and measured S-parameters of the proposed antenna are presented in Fig. 7. The measurement and simulation results are slightly different, which may be caused by assembly and processing errors. In both simulated and measured results, the return losses ( $|S_{11}|$ ,  $|S_{22}|$ , ...,  $|S_{66}|$ ) and isolation coefficients ( $|S_{21}|$ ,  $|S_{31}|$ , ...,  $|S_{61}|$ ) of all ports are better than 10 dB at 28–32 GHz.

Radiation patterns and gains of the antenna are shown in Figs. 8 and 9, respectively. As can be seen in Fig. 8, the simulated and measured radiation patterns are represented by solid lines and dashed lines, respectively. Good agreement can be observed

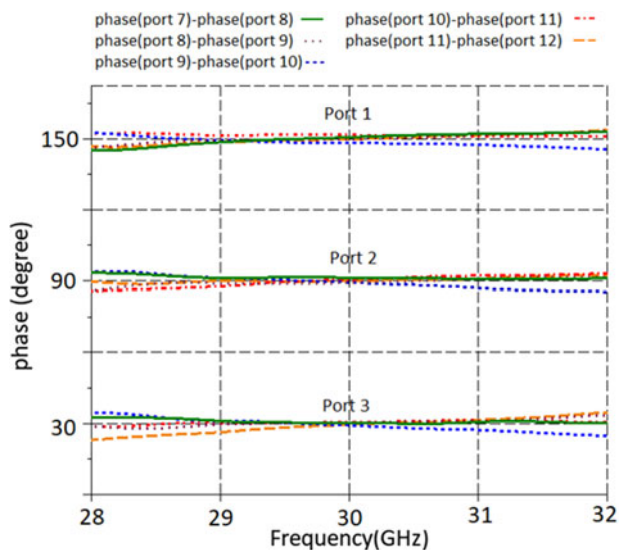


Figure 5. Phase differences of successive outputs when ports 1-3 are excited.

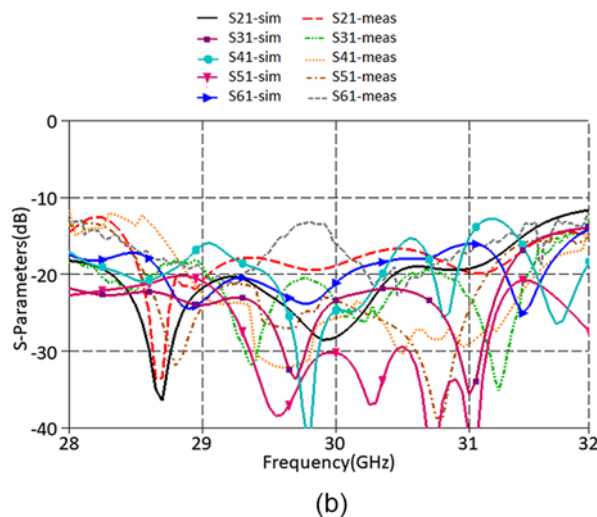
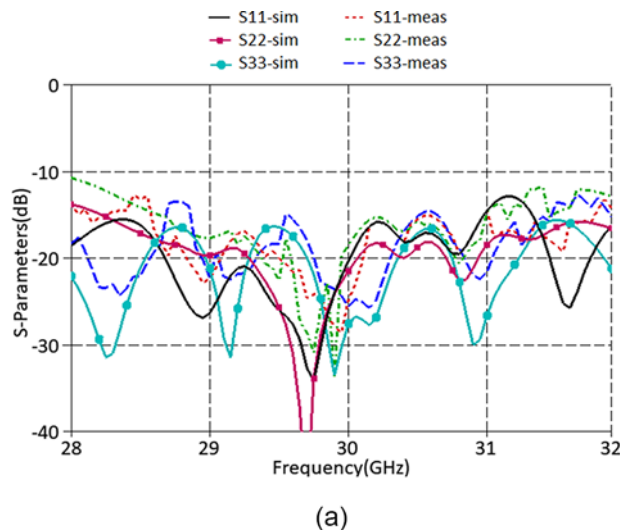
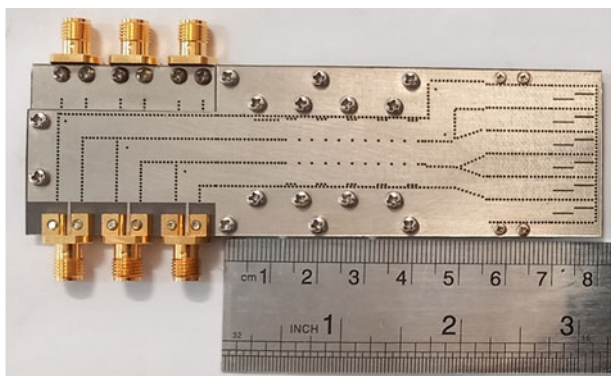
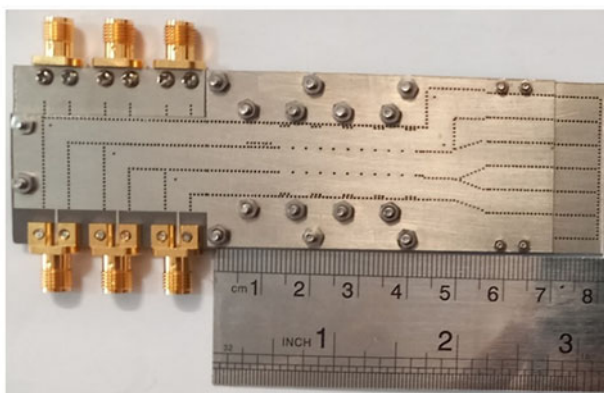


Figure 7. S-parameters of the proposed antenna: (a) reflection and (b) isolation.



(a)



(b)

Figure 6. The prototype of the two-layer six-beam antenna: (a) top view and (b) bottom view.

between simulation and measurement results. The antenna generates six beams in the directions of  $\pm 9^\circ$ ,  $\pm 30^\circ$ , and  $\pm 54^\circ$ . The six beams of the proposed antenna cover a switching range between  $-54^\circ$  and  $+54^\circ$ . The measured gains are around 11.8, 12.9, and 13.1 dBi for ports 1-3, respectively. In Table 3, the results of the proposed work are compared with other similar structures.

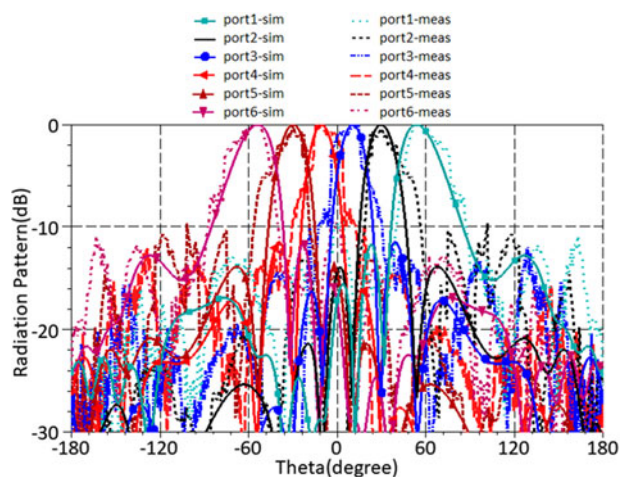
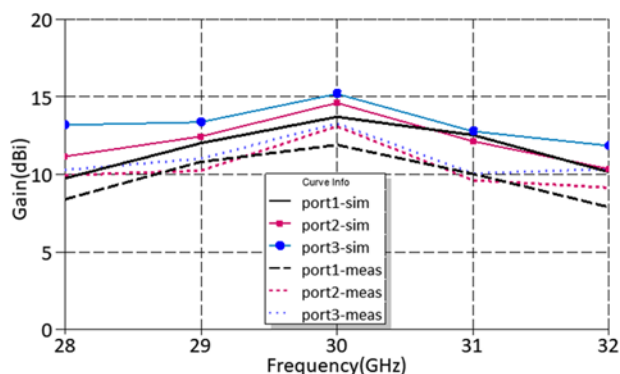


Figure 8. Simulated and measured radiation patterns of the antenna.

According to Table 3, due to the use of the SIW-MAC configuration, the proposed structure has a higher frequency bandwidth

**Table 3.** Comparison of the proposed structure with similar works

Reference	[19]	[2]	[34]	[35]	[30]	[32]	This work
Configurations	Rotman lens	Horn	Butler matrix	Butler matrix	Butler matrix	MAC	MAC
No. of beams	7	5	8	8	8	6	6
Bandwidth	3.5% 28–29 GHz	3.57% 27.5–28.5 GHz	7.14% 27–29 GHz	16.4% 56–66 GHz	10.1% 28–31 GHz	13.3% 28–32 GHz	13.3% 28–32 GHz
No. of layers	1	1	1	1	2	1	2
Angle coverage	100°	94°	110°	112°	110°	150°	154°
BFN area ( $\lambda_g^2$ )	$7 \times 7.87$	$3.3 \times 3$	$8.8 \times 10.6$	$15 \times 8$	$10 \times 4$	$10 \times 3.38$	$7.44 \times 3.38$

**Figure 9.** Simulated and measured gain of the antenna.

than papers [19] and [2], which have Rotman lens and horn configurations, respectively. Also, the coverage range of the proposed antenna is about 154°, which is more than the others. The size of the proposed BFN is  $72 \times 31.8 \times 0.787 \text{ mm}^3$ , which is reduced compared to similar works, especially reduced by 22% compared to the BFN in paper [32]. The total size of the two-layer six-beam antenna is  $82 \times 31.8 \times 0.787 \text{ mm}^3$  which can be a very suitable option for fifth and sixth generation communication applications. The proposed BFN consists of fewer components and a simpler design than similar works. Only 15 elements are used in this structure, while the structure presented in paper [32] consists of 23 elements. The proposed antenna creates six beams; however, the structure can also be extended for higher number of beams.

## Conclusion

In this paper, a compact two-layer six-beam antenna using  $3 \times 3$  MACs is designed, simulated, fabricated, and tested in the frequency range of 28–32 GHz that is suitable for 5G applications. The proposed antenna has the ability to generate six radiation beams, while its size is very compact compared to similar works. Six radiation beams in the bandwidth of 13.3% have been realized with stable beamforming performance. Due to the advantages of the proposed BFN such as the ability to create six radiation beams, compact structure, simple design, and good radiating performance, it would be an attractive candidate in 5G applications.

**Competing interests.** We have no conflicts of interest to disclose.

## References

- Rahimian A, Abbasi QH, Alomainy A and Alfadhl Y (2019) A low-profile 28-GHz Rotman lens-fed array beamformer for 5G conformal subsystems. *Microwave and Optical Technology Letters* **61**, 671–675.
- Lian J, Ban YL, Zhu JQ, Liu Y and Kang K (2018) SIW multibeam antenna based on modified horn beam-forming network. *IEEE Antennas and Wireless Propagation Letters* **17**, 1866–1870.
- Ashraf N, Haraz O, Ashraf MA and Alshebeili S (2015) 28/38-GHz dual-band millimeter wave SIW array antenna with EBG structures for 5G applications. In *2015 International Conference on Information and Communication Technology Research (ICTRC)*. Abu Dhabi.
- Hong W, Jiang ZH, Yu C, Zhou J, Chen P, Yu Z, Zhang H, Yang B, Pang X, Jiang M and Cheng Y (2017) Multibeam antenna technologies for 5G wireless communications. *IEEE Transactions on Antennas and Propagation* **65**, 6231–6249.
- Bogale TE and Le LB (2016) Massive MIMO and mmWave for 5G wireless HetNet: Potential benefits and challenges. *IEEE Vehicular Technology Magazine* **11**, 64–75.
- Numan AB, Frigon JF and Laurin JJ (2018) Printed S-Band multi-beam antenna with Luneburg lens-based beamforming network. *IEEE Transactions on Antennas and Propagation* **66**, 5614–5619.
- Tekkouk K, Ettorre M and Sauleau R (2018) SIW Rotman lens antenna with ridged delay lines and reduced footprint. *IEEE Transactions on Microwave Theory and Techniques* **66**, 3136–3144.
- Vashist S, Soni MK and Singhal PK (2014) A review on the development of Rotman lens antenna. *Chinese Journal of Engineering* **2014**, 1–9.
- Fonseca NJ (2009) Printed S-Band  $4 \times 4$  nolen matrix for multiple beam antenna applications. *IEEE Transactions on Antennas and Propagation* **57**, 1673–1678.
- Mosca S, Bilotti F, Toscano A and Vegni L (2002) A novel design method for Blass matrix beam-forming networks. *IEEE Transactions on Antennas and Propagation* **50**, 225–232.
- Chang CC, Lee RH and Shih TY (2009) Design of a beam switching/steering Butler matrix for phased array system. *IEEE Transactions on Antennas and Propagation* **58**, 367–374.
- Yang QL, Ban YL, Kang K and Wu G (2016) SIW multibeam array for 5G mobile devices. *IEEE Access* **4**, 2788–2796.
- Yang QL, Ban YL, Lian JW, Yu ZF and Wu B (2016) SIW butler matrix with modified hybrid coupler for slot antenna array. *IEEE Access* **4**, 9561–9569.
- Dall’Omo C, Monediere T, Jecko B, Lamour F, Wolk I and Elkael M (2003) Design and realization of a  $4 \times 4$  microstrip Butler matrix without any crossing in millimeter waves. *Microwave and Optical Technology Letters* **38**, 462–465.
- Djeraji T, Fonseca NJ and Wu K (2010) Design and implementation of a planar  $4 \times 4$  Butler matrix in SIW technology for wideband applications. In *The 40th European Microwave Conference*. Paris.
- Slomian I, Wincza K, Staszek K and Gruszczynski S (2017) Folded single-layer  $8 \times 8$  Butler matrix. *Journal of Electromagnetic Waves and Applications* **31**, 1386–1398.

17. **Cerna RD and Yarleque MA** (2018) A 3D compact wideband  $16 \times 16$  Butler matrix for 4G/3G applications. In *IEEE/MTT-S International Microwave Symposium-IMS*. Philadelphia.
18. **Yang Q, Gao S, Luo Q, Wen L, Ren X, Wu J, Ban YL and Yang X** (2019) A low complexity  $16 \times 16$  butler matrix design using eight-port hybrids. *IEEE Access* 7, 177864–177873.
19. **Cheng YJ, Hong W, Wu K, Kuai ZQ, Yu C, Chen JX, Zhou JY and Tang HJ** (2008) Substrate integrated waveguide (SIW) Rotman lens and its Ka-band multibeam array antenna applications. *IEEE Transactions on Antennas and Propagation* 56, 2504–2513.
20. **Cheng YJ, Hong W and Wu K** (2010) Design of a substrate integrated waveguide modified R-KR lens for millimetre-wave application. *IET Microwaves, Antennas & Propagation* 4, 484–491.
21. **Yang QL, Ban YL, Lian JW, Zhong LH and Wu YQ** (2017) Compact SIW  $3 \times 3$  Butler matrix for 5G mobile devices. In *International Applied Computational Electromagnetics Society Symposium (ACES)*. Suzhou.
22. **Gong RJ, Ban YL, Lian JW, Liu Y and Nie Z** (2019) Circularly polarized multibeam antenna array of ME dipole fed by  $5 \times 6$  Butler matrix. *IEEE Antennas and Wireless Propagation Letters* 18, 712–716.
23. **Lian JW, Ban YL, Xiao C and Yu ZF** (2018) Compact substrate-integrated  $4 \times 8$  Butler matrix with sidelobe suppression for millimeter-wave multibeam application. *IEEE Antennas and Wireless Propagation Letters* 17, 928–932.
24. **Lian JW, Ban YL, Zhu JQ, Kang K and Nie Z** (2018) Compact 2-D scanning multibeam array utilizing the SIW three-way couplers at 28 GHz. *IEEE Antennas and Wireless Propagation Letters* 17, 1915–1919.
25. **Pezhman MM, Heidari AA and Ghafoorzadeh-Yazdi A** (2020) Compact three-beam antenna based on SIW multi-aperture coupler for 5G applications. *AEU-International Journal of Electronics and Communications* 123, 153302.
26. **Pezhman MM and Heidari AA** (2019) Design of compact SIW-based multi-aperture coupler for Ku-band applications. In *27th Iranian Conference on Electrical Engineering (ICEE)*, Yazd.
27. **Pezhman MM, Heidari AA and Ghafoorzadeh-Yazdi A** (2021) A compact  $4 \times 4$  SIW beamforming network for 5G applications. *AEU-International Journal of Electronics and Communications* 135, 153714.
28. **Kim S, Yoon S, Lee Y and Shin H** (2019) A miniaturized Butler matrix based switched beamforming antenna system in a two-layer hybrid stackup substrate for 5G applications. *Electronics* 8, 1232.
29. **Li X, Cai M, Shen H and Yang G** (2017) A compact two-dimensional multibeam antenna fed by two-layer SIW Butler matrix. In *IEEE International Symposium on Antennas and Propagation & USNC/URSI National Radio Science Meeting*. San Diego.
30. **Zhong LH, Ban YL, Lian JW, Yang QL, Guo J and Yu ZF** (2017) Miniaturized SIW multibeam antenna array fed by dual-layer  $8 \times 8$  Butler matrix. *IEEE Antennas and Wireless Propagation Letters* 16, 3018–3021.
31. **Balanis CA** (2016) *Antenna Theory: Analysis and Design*. New Jersey: John Wiley & Sons.
32. **Pezhman MM, Heidari AA and Ghafoorzadeh-Yazdi A** (2016) A novel single layer SIW  $6 \times 6$  beamforming network for 5G applications. *AEU-International Journal of Electronics and Communications* 155, 154380.
33. **Bembarka A, Setti L, Tribak A, Tizyi H and El Ouahabi M** (2023) A novel wideband beamforming antenna for 5G applications by eliminating the phase shifters and crossovers from the Butler matrix. *Progress in Electromagnetics Research C* 133, 51–63.
34. **Idrus II, Latef TA, Aridas NK, Talip MSA, Yamada Y, Izam TFTMN and Rahman TA** (2020) Design and characterization of a compact single-layer multibeam array antenna using an  $8 \times 8$  Butler matrix for 5G base station applications. *Turkish Journal of Electrical Engineering and Computer Sciences* 28, 1121–1134.
35. **Li Y and Luk KM** (2016) A multibeam end-fire magnetoelectric dipole antenna array for millimeter-wave applications. *IEEE Transactions on Antennas and Propagation* 64, 2894–2904.



**Mohammad Mahdi Pezhman** received the B.Sc. degree from the Shahid Bahonar University of Kerman, Kerman, Iran, in 2012. He received the M.Sc. degree in electrical engineering at the Kerman Graduate University of Technology, Kerman, Iran, in 2015, and the Ph.D. degree in electrical engineering, communication (field and wave) from Yazd University, Yazd, Iran, in 2021. Currently, he is working at the Department of Electrical and Computer Engineering of Vali-e-Asr University of Rafsanjan, Rafsanjan, Iran. His research interests include active and passive microwave devices and circuits, distributed amplifiers, 5G beamforming networks, and multi-beam SIW antennas.



**Abbas Ali Heidari** was born in Yazd, Iran, in 1970. He received the B.Sc. degree from Shahid Bahonar University of Kerman, Kerman, Iran, in 1993, and the M.Sc. and Ph.D. degrees in electrical engineering from Tarbiat Modarres University, Tehran, Iran, in 1996 and 2003, respectively. Currently, he works as a professor of Yazd University, Yazd, Iran, where he served as the head of the Electrical Engineering Department from 2004 to 2006 and dean of the E-learning and Open Learning Center from 2007 to 2010. He served as the head of the Technology Affairs from 2014 to 2016, and head of the Communication Engineering Department from 2016 to 2018. His research interests include microstrip antennas, SIW and metamaterial-based antennas, microwave absorbers, and passive microwave components.



**Ali Ghafoorzadeh-Yazdi** was born in Yazd, Iran, in 1965. He received the B.Sc. degree from the University of Tehran, Tehran, Iran, in 1988, and the M.Sc. and Ph.D. degrees in electrical engineering from Tarbiat Modares University, Tehran, Iran, in 1997 and 2009, respectively. Currently, he works as an associate professor with the Department of Electrical Engineering, Yazd University, Yazd, Iran. His current research interests include the theory and design of antennas, array antennas, microwave

passive components, and computational electromagnetics.



**Fatemeh Homayoon** received the B.S. degree in electrical engineering from O.T.F. University, Fars, Iran, in 2012, and the M.S. degree in electrical engineering from the University of Sistan and Baluchestan, Sistan and Baluchestan, Iran, in 2015. Currently, she is the Ph.D. student at the Department of Electrical Engineering at Yazd University, and her research interests are in the design of RF and microwave devices, antennas and propagation, metamaterials, and

microwave plasmonics.



**Hamed Shahraki** was born in Zabol, Iran, in 1984. He received B.Sc. in electrical engineering from University of Sistan and Baluchestan, Zahedan, Iran, in 2008, M.S. in electrical engineering from Shiraz University of Technology, Shiraz, Iran, in 2012, and Ph.D. degree from Shahid Bahonar University of Kerman, Kerman, Iran, in 2018. He is currently working as an assistant professor with the Department of Electrical Engineering, Velayat University of Iranshahr, Iranshahr, Iran. His main areas of research interest include MTM and RF/microwave circuits design.